Synthesis and Some Solution Properties of Poly(γ-stearyl α,L-glutamate)†

D. S. Poché,*,‡ W. H. Daly, and P. S. Russo

Department of Chemistry and Macromolecular Studies Group, Louisiana State University, Baton Rouge, Louisiana 70803

Received November 21, 1995; Revised Manuscript Received June 2, 1995®

ABSTRACT: The synthesis of poly(γ-stearyl L-glutamate) is reported, starting from glutamic acid. The γ-stearyl L-glutamate amino acid (SLGAA) was prepared from stearyl alcohol and L-glutamic acid. Ring closure of SLGAA to the cyclic *N*-carboxyanhydride (NCA) monomer was accomplished using bis-(trichloromethyl) carbonate (triphosgene). Polymerization of the SLGNCA monomer in the presence of either primary amines or sodium methoxide produced a series of polypeptides with molecular weights ranging from 20 000 to 300 000. The polydisperse polymers were characterized by static and dynamic light scattering, solution viscometry, ^{1}H and ^{13}C NMR, and infrared spectroscopy. The polymer was also modeled using the SYBYL molecular graphics package. The combined data indicate a semiflexible structure, with PSLG side chains being well extended from the polymer backbone in the good solvent, tetrahydrofuran. Gel permeation chromatography and dynamic light scattering data indicated polydispersity ratios (M_w/M_n) in the range of 1.1–2.0. The Mark–Houwink–Sakurada coefficients obtained were $K = (1.26 \pm 0.3) \times 10^{-5}$ cm^3/g and $a = 1.29 \pm 0.09$ for M_w in the range of 38 000–250 000. The hydrodynamic diameter of the PSLG rod was calculated to be 3.7 ± 0.2 nm; the diameter of mutual exclusion calculated from the Zimm–Schulz–Onsager equation was 3.6 ± 0.7 nm. These values were in good agreement with the value obtained from the SYBYL molecular model.

Introduction

Synthesis of poly(alkyl L-glutamate)s provides a novel type of semiflexible polymer for fundamental study, especially for the understanding of rodlike polymer behavior in solution. Like the polyisocyanates,[1–9] poly(alkyl L-glutamate)s derive their stiffness from the formation of a helical backbone in heliogenic solvents. While many rod-like polymers are intractable or poorly soluble,[10] the long side chains of the poly(alkyl L-glutamate)s impart both solubility and reduced melting temperatures to the polymers. They can be synthesized readily from the *N*-carboxyanhydride (NCA) monomers[11–19] to produce high molecular weight polypeptide homopolymers or copolymers. Many reports[20–22] on the polymerization of an NCA to a high molecular weight homopolymer have been published. Indeed, polymerization of γ-stearyl L-glutamate *N*-carboxyanhydride (SLGNCA) produced α-helical poly(stearyl α,L-glutamate) (PSLG) in a range of molecular weights. Several of the literature reports[23–26] on PSLG have described its ability to form thermotropic liquid crystals. However, PSLG used in these studies was obtained by transesterification of commercially available poly(γ-benzyl α,L-glutamate) (PBLG) or poly(γ-methyl α,L-glutamate) (PMLG) with stearyl alcohol. Incomplete transesterification yields copolymers that are likely to be unsuitable for many fundamental studies. Details of the synthesis from monomer, analytical characterization, and solution properties of PSLG have been lacking even though the polymer is expected to exhibit some unique solution properties compared to the more completely characterized PBLG and PMLG. Besides imparting thermotropic liquid crystalline behavior in the melt, the long, aliphatic side chains also provide solubility in many organic solvents that support the α-helix. The side chains may also help provide miscibility with other polymers in blends. In short, PSLG is an appealing system for fundamental studies of solution and gel behavior of rodlike polymers and also for compatibility studies with less rigid polymers.[27] We report here some details on the synthesis of PSLG starting from its parent α-amino acid and its behavior in solution as elucidated by static and dynamic light scattering (SLS and DLS) and NMR.

† Presented in part at the Dallas ACS National Meetings, April 1989, and the Baton Rouge ACS Southwest Regional Meeting, Dec 1989.

‡ Present address: Department of Chemistry and Physics, Southeastern Louisiana University, Hammond, LA 70402.

® Abstract published in *Advance ACS Abstracts,* August 1, 1995.

Experimental Section

Reagents. All solvents and reactants were reagent grade except those employed in polymerization reactions. NCA polymerization solvents either were dried over molecular sieves prior to use or were of Aldrich Chemical Co. Gold Label purity. Any solvent contacting SLGNCA was dried over 4 Å from molecular sieves at least overnight prior to use. Bis-(trichloromethyl) carbonate (triphosgene) was prepared by exhaustive chlorination of dimethyl carbonate.[12,28] All polymerization flasks were flame dried prior to use, and moisture was excluded during polymerizations with calcium sulfate drying tubes.

γ-Stearyl α,L-Glutamate. See Wasserman *et al.*[29] Yield: 12.2 g (56%). Mp: 165–167 °C. IR: 2830 (aliphatic CH_2), 1725 (COOR), 1590 (COOH) cm^{-1}.

γ-Stearyl α,L-Glutamate *N*-Carboxyanhydride. γ-Stearyl α,L-glutamate (10 g, 0.0251 mol) was suspended in THF (150 mL), and the reaction flask was fitted with a condenser which was vented into concentrated ammonium hydroxide to trap HCl or phosgene gas. After warming to 50 °C, 1/3 of an equivalent of triphosgene (2.52 g, 0.0085 mol) was added as a single aliquot. The reaction slurry usually became homogeneous within 1 h. After about 1 h, the reaction was concentrated to about 1/3–1/2 of its original volume under vacuum and poured into twice its volume of hexane. Crystallization began immediately upon mixing with hexane. After overnight refrigeration, the crystals were recovered by suction filtration and the solid redissolved in chloroform or dichloromethane. This solution was filtered through a cake of Celite after first shaking with a small amount of sodium carbonate. The filtrate was concentrated, poured into hexane, and refrigerated. The recrystallization step was repeated twice. Mp: 77–78 °C. Yield was typically 85–90%. ^{1}H NMR: δ 0.87 (t, terminal CH_3), 1.25 (s, CH_2 groups in the stearyl chain), 2.19 (m, β-CH_2),

0024-9297/95/2228-6745$09.00/0

Table 1. Reaction Conditions for Various SLGNCA Polymerizations

monomer conc,[a] w/v %	{M}:{I} ratio	yield, %	[η], dL/g	degree of polymerization
30.0	200[b]	92	0.15	123
15.0	100	95	0.64	392
5.0	200	90	0.20	157
4.5	100	95	0.83	445
4.5	300	84	0.33	340
2.0	200, 100	90	1.13	650
10.0	100[d]	90	0.10	65

[a] Typical reaction conditions: dichloromethane solvent stirred for 5 days at ambient temperature. [b] Initiator: sodium methoxide in methanol unless otherwise noted. [c] Reaction spiked with another aliquot of initiator after 24 h. [d] Initiator: benzylamine.

2.55 (t, γ-CH_2), 4.09 (t, CH_2 in the side chain adjacent to γ-ester), 4.39 (t, α-CH), 6.75 (brs, NH). IR: 2980 (str., aliphatic CH_2), 1830, 1810 (anhydride carbonyls) cm^{-1}.

Poly(γ-stearyl α,L-glutamate). (A) Primary Amine Initiation. SLGNCA (1.0 g, 0.0023 mol) was dissolved in dichloromethane (DCM; 50 mL), and benzyl amine (128 μL of a 2% (v/v) stock solution in DCM, {M}:{I} = 100) was added to the stirred monomer solution. After 3 days at room temperature, the solvent volume was reduced to 10 mL and the polypeptide was precipitated into acetone (100 mL). The product was recovered by gravity filtration and vacuum dried at room temperature.

(B) Methoxide Initiation. SLGNCA (1.0 g, 0.0023 mol) was dissolved in DCM (25 mL) before sodium methoxide (5.4 μL of a 25% solution in methanol) was added at once to the stirred solution. After standing for 5 days, the polymer was precipitated by pouring the concentrated reaction medium into acetone. Typical yields of polymer exceeded 90% in both of the above cases; see Table 1. Mp: 60 °C. IR: 3290 (NH amide), 2850 (aliphatic CH_2), 1660 (CONH), 1550 (CONH) cm^{-1}. See Figure 6a–c for ^1H and ^{13}C spectra.

Transesterification of PMLG. A solution of PMLG (20 g of a 10% solution, i.e., 2 g of polymer, 0.014 mol of monomer) in 70:30 ethylene dichloride/ethylene tetrachloride was diluted with 50 mL of the same solvent mixture. *p*-Toluenesulfonic acid (2.3 g, 0.012 mol) and stearyl alcohol (32.4 g, 0.12 mol) were added, and the reaction was heated and stirred at 65 °C for 5 days. The reaction was then poured into 1 L of acetone to precipitate the polymer. Repeated precipitations of the polymer from DCM solutions removed unreacted stearyl alcohol. The material was vacuum dried and found to be 94% transesterified by weight gain. ^1H NMR indicated a 85–90% substitution of the methyl groups. The IR spectrum was identical to the PSLG synthesized from the monomer. No hydroxyl group due to unreacted stearyl alcohol was found in the IR spectrum.

Characterization. IR spectra were recorded on a Perkin-Elmer 83E spectrometer. NMR spectra were recorded on IBM Bruker AR-100 100-MHz or IBM Bruker 200-MHz instruments using tetramethylsilane as an internal standard. Intrinsic viscosity measurements were measured in a constant-temperature water bath at 30 °C in THF using an Ubbelohde capillary viscometer. Solvent flow time exceeded 100 s. When necessary, solutions were filtered through a 0.45-μm (Nalge) syringe filter. The values of [η] were obtained from the standard Huggins plot interpretation. GPC data were collected on a Waters HPLC instrument equipped with a Phenogel 10-μm mixed-bed column. A differential refractive index detector was used to detect the column eluent. A precolumn was used to trap particular matter in the mobile phase, THF containing toluene as an internal standard, which was pumped at 1 mL/min. An injection volume of 25 μL of 5% (w/v) solutions was used. The data was collected and analyzed using Nelson 2600 GPC software.

The specific refractive index increment, d*n*/d*c*, for PSLG in THF was measured at 25 °C, and $\lambda_0 = 488.0$ nm over the same concentration range studied in the light scattering experiments using a Brice–Phoenix differential refractometer fitted and recalibrated for laser line operation.[30] The value obtained for PSLG in THF, assuming no dependence on molecular weight, is d*n*/d*c* = 0.080 ± 0.002 mL/g. The light scattering instrument used a tunable Lexel Model 95 argon ion laser. For SLS experiments, the 488.0-nm line was selected. For DLS experiments, the 514.5-nm line was used. A Lauda RM-6 water bath circulated constant-temperature water through an insulated copper block in which the sample cell rested. An EMI-9863 phototube was connected to a Precision Pacific Model 126 photometer which, in turn, fed photopulses to a 272-channel Langley–Ford Model 1096 operating in linear mode. For light scattering, HPLC-grade tetrahydrofuran (THF; Baker analyzed reagent) was used. It is low in water content (less than 0.05%) and contains low particulate matter. Light scattering cells were cleaned and tested by observing the laser beam using the 100× ocular on the instrument. Polymer stock solutions were made by filtering THF into a flask containing weighed PSLG under a blanket of nitrogen using a 0.02-μm Anopore syringe filter. The stock solution was then filtered into a dust-free test tube using a 0.2-μm poly(tetrafluoroethylene) (PTFE) filter (Gelman). Dilutions were made with 0.02-μm Anopore filtered THF. Stock solution and solvent were centrifuged for no less than 1 h (sometimes overnight) at 9000*g* prior to dilutions directly into cleaned cells, the dilutions being performed under a blanket of nitrogen. These solutions were measured after centrifuging at 9000*g* for no less than 1 h (sometimes overnight). Raw intensity data from DLS were analyzed by the method of cumulants.[31] SLS data were obtained by evaluating Zimm plots generated from the average scattering intensity at eight angles and five concentrations of polymer solution.

Discussion

SLGAA and SLGNCA Synthesis. Selective esterification of the γ-carboxylic acid position of L-glutamic acid with long-chain hydrocarbon alcohols is not straightforward. The insolubility of L-glutamic acid in most organic solvents, the difficulty of removing excess stearyl alcohol, and the purification of the resulting SLGAA make its synthesis unwieldy. Several approaches were attempted,[32–34] a few of which have proved successful in the synthesis of γ-benzyl L-glutamate (BLGAA).[35,36] Most methods were unsuitable for producing SLGAA, although modest success was achieved through the esterification of *N*-phthaloyl L-glutamic acid[34] and subsequent deblocking of the amino function. By far the most efficient method for specifically producing SLGAA was that of Wassermann *et al.*[29] The success of this method lies both in the use of the sulfuric acid catalyst and the *tert*-butanol solvent medium. This approach to SLGAA from L-glutamic acid has proven effective because (1) the sulfuric acid catalyst aids in blocking the α-carbonyl from attack, (2) hot *tert*-butanol is an effective solvent medium for all the reactants and the resulting product, and (3) the product can be recrystallized cleanly from 1:1 n-butanol/water, giving a product pure enough for direct conversion to the NCA monomer. SLGAA is not readily soluble in organic solvents (at room temperature) and is insoluble in water.

The SLGNCA was produced initially by the Fuchs–Farthing method,[17,18a,b] but this process was subsequently replaced by the method of Daly and Poché[12] where bis(trichloromethyl) carbonate (triphosgene) was used as a phosgene gas substitute. Triphosgene was first[37] reported in the 1880s; more recently, Eckert and Forster[28] evaluated it as a general phosgene substitute. Using an approach similar to Eckert and Forster, triphosgene was synthesized by exhaustive chlorination of dimethyl carbonate. The details of its utility in producing the NCA derivative of an α-amino acid are

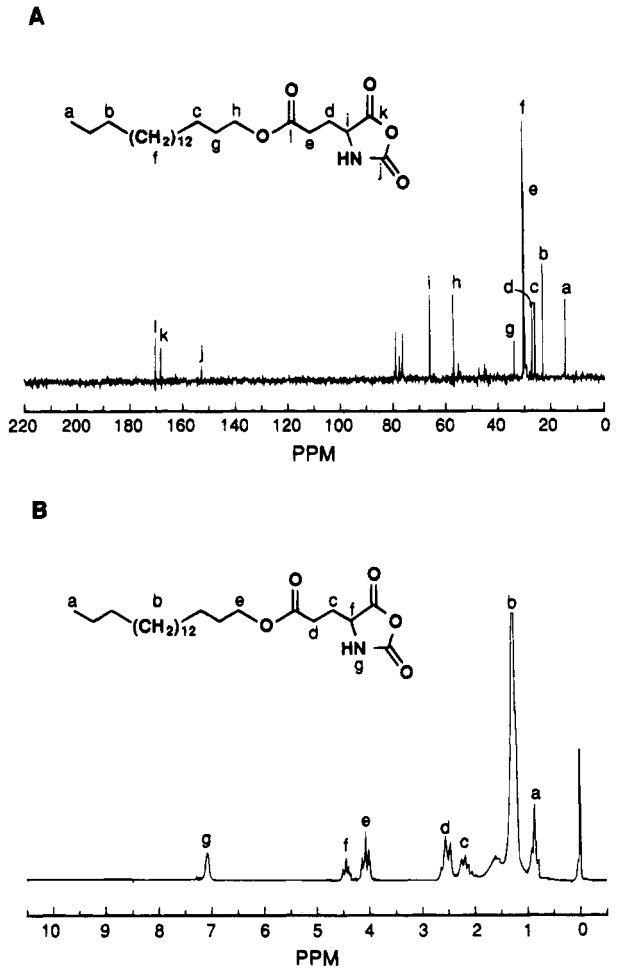

Figure 1. NMR spectra of SLGNCA. Solvent was $CDCl_3$ with TMS standard. (A) 25-MHz ^{13}C; (B) 100-MHz ^1H.

published elsewhere.[12] Parts A and B of Figure 1 show the ^{13}C and ^1H NMR spectra of the SLGNCA monomer, respectively. The spectral assignments shown on the figures are consistent with the expected structure. While some NCA derivatives of α-amino acids are isolated as oils, SLGNCA is easily recrystallized from hexane, yielding white, leafy crystals. SLGNCA has a low melting point temperature and, like most NCA derivatives, it is moisture and heat sensitive.

Synthesis of the Polymer. NCA polymerizations are usually[38-51] initiated by primary amines or by a strong base such as sodium methoxide or a tertiary amine. It is generally accepted that primary amine initiations lead to polymers with narrower molecular weight distributions (Poisson distribution), with the molecular weight predictable by the monomer/initiator ratio and with the initiator covalently bound to the polymer chain it initiates. Although a comparatively narrow MWD can be expected from primary amine initiation, the monomer/initiator ratio generally cannot exceed about 100 or the polymerization becomes prohibitively slow,[35] leading to unequal rates of chain initiation and products with a broader MWD. Strong base initiation can yield much higher molecular weight polymers. The mechanism proposed for this process involves an abstraction of the acidic hydrogen on the nitrogen in the NCA ring, forming an "active monomer", which can then react as a nucleophile by attacking an NCA at the C5 position. Ring opening followed by loss of carbon dioxide produces an amino group that will attack sequential NCA's and thus lead to chain extension. Active monomer initiation leaves an NCA ring at the end of a growing polymer chain; as the polymerization proceeds, the concentration of monomeric NCA's is reduced to the point that the enchained NCA ring competes for the growing free amino end of another chain and chain coupling occurs. The coupling process is very effective in enhancing the molecular weight, but it also increases the polydispersity of the polypeptide.

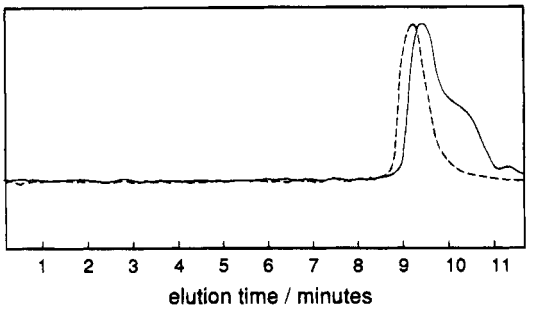

Figure 2. Typical GPC trace of primary amine initiated SLGNCA: (solid line) 2% initial monomer concentration; (dashed line) 5% initial monomer concentration. Little, if any, difference was noted in the GPC trace when increasing the initial monomer concentration in the reaction from 5 to 25% (w/v).

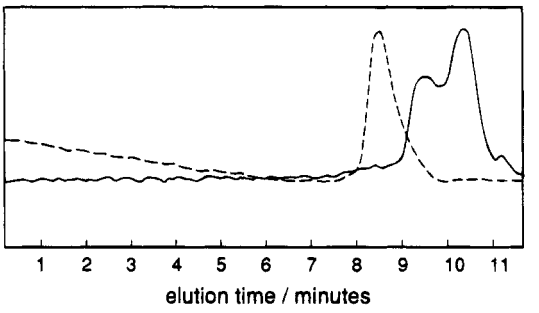

Figure 3. GPC traces of a sodium methoxide initiated polymerization: (solid line) 2.5 days of reaction; (dashed line) 5 days of reaction.

Both primary amine and strong base initiation of the SLGNCA monomer was used to produce the PSLG polymers, as shown in Table 1. The strong base (sodium methoxide) initiated polymers had the higher molecular weights. Figure 2 is a typical GPC result obtained for primary amine initiation. When SLGNCA is initiated with benzylamine at a monomer/initiator ratio ({M}:{I}) of 100 and a monomer concentration of at least 5% (w/v), increasing the initial monomer concentration had little effect on the molecular weight or MWD of the polymer. Dropping the initial monomer concentrations as low as 2% (w/v), however, led to an unequal rate of chain initiation/chain growth, causing a broad MWD and lower molecular weight polymer. We also found, as earlier literature[52] suggests, that "aging" of a strong base initiated NCA polymerization leads to an enhancement of the molecular weight. As Figure 3 shows, the GPC trace of a sodium methoxide initiated reaction allowed to run 2 days indicates a polymer with a bimodal MWD. A reaction proceeding for 5 days at the same initial monomer and initiator concentration resulted in a higher molecular weight polymer, but the MWD is still greater than that observed for polymers obtained via primary amine initiation. The sodium methoxide was added in a solution of methanol to the reactions. The methanol itself could initiate chains, but its reaction with SLGNCA is undoubtedly much slower than attack by growing amino chain ends.[53] The highest molecular weight polymers produced for this

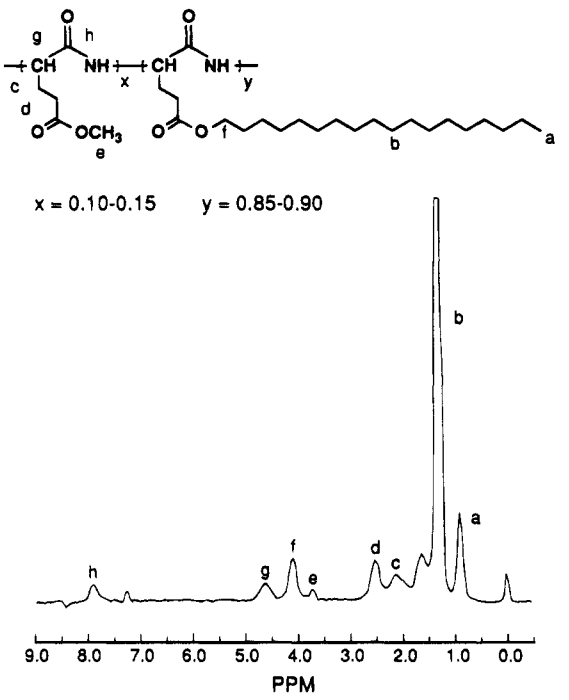

Figure 4. 100-MHz ^{1}H NMR spectrum of PSLG-EX.

study were typically prepared from 5–10% (w/v) monomer solutions in DCM initiated by sodium methoxide in methanol at {M}:{I} ≥ 100. As shown by the intrinsic viscosity data in Table 1, however, higher {M}:{I} ratios alone will not guarantee the highest molecular weight polymers. The initial monomer concentration in the reaction must be higher with increasing {M}:{I} ratios. For example, a reaction containing an initial monomer concentration of 2% (w/v) was stirred with MeO^- at a {M}:{I} = 200. After about 1 day of reaction, no measurable polymerization had begun (by IR). The reaction was then "spiked" with another aliquot of MeO^-, causing the polymerization to proceed. In another reaction, at an initial monomer concentration of 4.5% (w/v) MeO^- was added at a {M}:{I} = 300. Even though the polymerization proceeded, the yield of the resulting polymer was reduced.

PSLG can also be prepared by derivatizing a commercially available poly(γ-alkyl α,L-glutamates) such as poly(γ-benzyl α,L-glutamate) (PBLG; Sigma Chemical Co.) or poly(γ-methyl α,L-glutamate) (PMLG; Polysciences, Inc.) by transesterification with stearyl alcohol. Literature reports[23,54] of high degrees of transesterification suggest a good synthetic route to PSLG. However, it is difficult to obtain 100% transesterified material. We reacted PMLG with an excess of stearyl alcohol, catalyzed with *p*-toluenesulfonic acid (*p*-TSA) for 5 days and found by ^{1}H NMR that only about 85–90% of the methyl groups had been displaced. Figure 4 shows the NMR trace for the transesterified material, hereafter referred to as PSLG-EX. Note the presence of the peak at 3.8 ppm due to unsubstituted methyl ester groups. Other workers have reported a similar degree of transesterification. In essence, the reaction outlined above produces a 9:1 SLG/MLG copolymer as the product. These results emphasize the importance of producing PSLG directly from the monomer for elucidating certain features of its structure and physical behavior. Transesterification is a convenient technique for producing glutamate copolymers, but it should not be considered a suitable synthesis for pure homopolymers—neither should the product be considered a suitable substitute for the pure homopolymer in physical characterization studies.

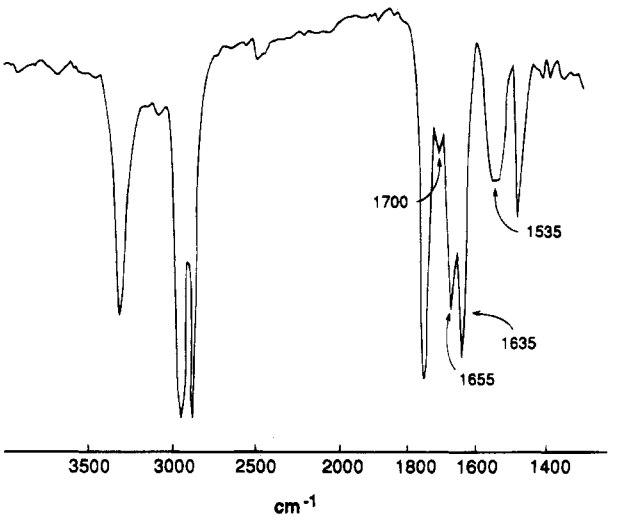

Figure 5. IR trace of PSLG predominately in the β-sheet conformation.

We were also able to produce a large fraction of PSLG in a β-sheet form by reaction of a 40% (w/v) solution of SLGNCA in DCM with tributylamine at a {M}:{I} = 30. The monomer appeared incompletely soluble at this concentration—the initiator was added to the suspension. Figure 5 shows an IR spectrum of the material; the band positions due to the backbone amide at 1700, 1635, and 1535 cm^{-1} indicate the β-sheet form of a polypeptide.[55] The PSLG samples used in the physical characterization discussed below showed no evidence of these IR bands but rather displayed bands typical of an α-helical conformation (CONH bands at 1660 and 1550 cm^{-1}).

NMR Characterization. A ^{1}H NMR spectrum (Figure 6a) of PSLG shows considerable overlap of the β-CH_2 and γ-CH_2 peaks and overlap of the α-CH with the CH_2O peak of the side chain when the backbone is in the helical conformation. If the helix is broken with a reagent that interrupts the intramolecular hydrogen bonds, such as trifluoroacetic acid (TFA), the peaks in the ^{1}H NMR spectrum become more clearly resolved (Figure 6b). Note that, after addition of TFA, the β-CH_2 and γ-CH_2 peaks are resolved and that the α-CH peak shifts to 4.6 ppm. In a similar manner, the peaks in the PSLG ^{13}C NMR spectrum also become easier to detect and more cleanly resolved, as parts C and D of Figure 6 show. The α-CH, the carbonyl in the backbone of the polymer, and the β- and γ-carbons are not discernable in the spectrum until addition of TFA.

In a ^{1}H NMR spectrum of high molecular weight poly(α,L-glutamates), the chemical shift of the α-CH is useful in determining the secondary conformation of the polymer chain. In PSLG the α-CH peak is poorly resolved and is located at about 3.9 ppm when in the α-helix conformation. Upon the addition of a helix-breaking reagent, the peak sharpens and shifts to about 4.6 ppm. The presence of both conformations in solution will exhibit peaks at both positions. The peak assignments mentioned above are consistent with observations[56,57] of the α-CH in PBLG. Because of the correlation of the α-CH chemical shift with secondary conformation, ^{1}H NMR can be used to follow the helix–coil transition as increasing amounts of TFA are added to the PSLG/$CDCl_3$ solution; 5.6–6.5% TFA is required to completely disrupt the helix conformation in a 10%

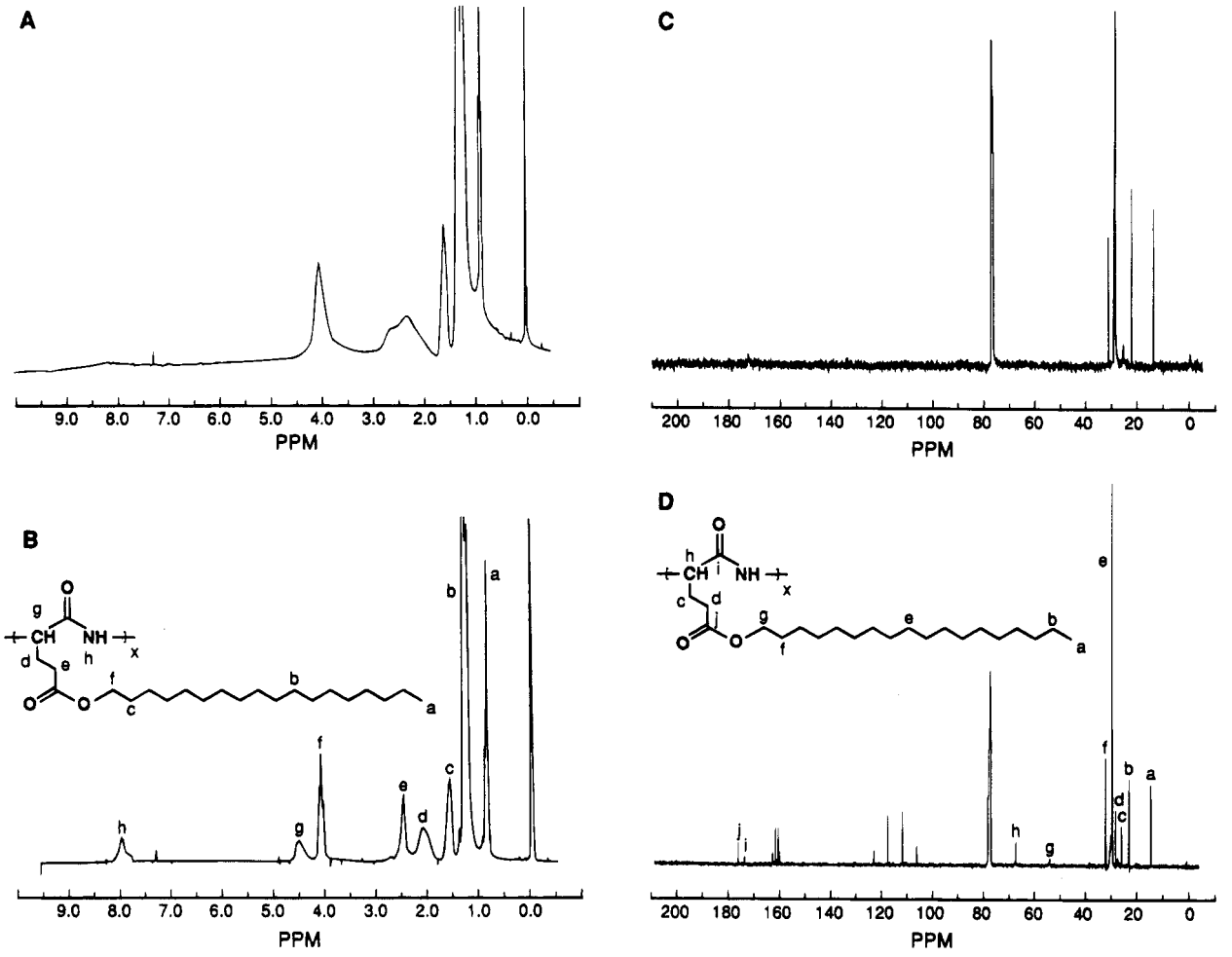

Figure 6. NMR spectra of PSLG run in $CDCl_3$ with TMS standard. Quartets at about 115 and 160 ppm are due to TFA. (A) 200-MHz ^1H NMR without trifluoroacetic acid (TFA); (B) 200-MHz ^1H NMR with 10% TFA; (C) 50-MHz ^{13}C NMR without trifluoroacetic acid (TFA); (D) 50-MHz ^{13}C NMR with 10% TFA.

(w/v) PSLG in $CDCl_3$ (M_w = 20 000). Smith and Woody[58] followed the helix–coil transition of poly(γ-dodecyl L-glutamate) (PDLG; M_w = 25 000) by TFA addition using optical rotatory dispersion and found that complete conversion occurred at 6% TFA.

Solution Characterization. The present solution studies were undertaken in support of the synthetic effort; they are of limited use for physical characterization, due to sample polydispersity. It is hoped that these preliminary results will serve in good stead until more nearly monodisperse samples can be analyzed. This section begins with properties from static light scattering, viscometry, and molecular modeling. The polydispersity question is considered using GPC and some special properties of SLS for rods. Finally, dynamic light scattering is applied.

The weight-average molecular weight, M_w, the osmotic second virial coefficient, A_2, and the radius of gyration, R_g, were determined by static light scattering (SLS). Table 2 summarizes these and other results. The diameter of mutual exclusion can be calculated by use of the Onsager–Zimm–Schulz[59] relationship for A_2, given in eq 1 where N_A is Avogadro's number, L is the

$$A_2 = \pi N_A d L^2/(4M^2) \qquad (1)$$

length of a rod of molecular weight M, and d is the thermodynamic diameter (i.e., the diameter based on mutual exclusion of rods). The virial coefficient of a thin rod does not depend on M. Figure 7 confirms the absence of any systematic trend for PSLG. The value of d obtained from eq 1 depends on how L is computed. Assuming the translation per monomer repeat along the α-helical axis is h = 0.15 nm, L can be computed as $0.15M_w/M_0$, where M_0 = 382 is the residue molecular weight. The length may also be computed as $L_{R_g} = 12^{1/2}R_g$. These lengths and associated diameters appear in Table 2. The difference in the lengths obtained reflects the polydispersity of the present samples and greatly limits the precision with which d can be obtained. The thermodynamic diameter can only be estimated as 3 ± 1 nm, considering all the data. However, the average result using $L_{R_g} = 12^{1/2}R_g$ and d_{R_g} = 2.3 ± 0.6 nm is probably low. A higher average than the weight average should be used in conjunction with the z-average of the square of the radius of gyration, which is what light scattering measures in a polydisperse sample. For rods, the correct average is the geometric mean of M_z and M_{z+1},[60] and this is not known. Using $L = 0.15M_w/M_0$ is more reasonable, since a weight-average length is compared to a weight-average mass. The requisite assumption—that h = 0.15 nm—can be shown to be reasonable; see below. The average diameter using $L = 0.15M_w/M_0$ is d = 3.6 ± 0.7 nm.

Equation 2 can be used[61] to calculate a density-based reference diameter, d_ϱ, where ϱ is the polymer density, assumed to be the inverse of the partial specific volume, v = 1.024 ± 0.008 mL/g, measured in THF using a Paar densitometer. The density-based diameter is d_ϱ = 2.3

Table 2. Summary of Data Obtained for Linear PSLG from SLS, DLS, and Viscometry

$M_w/10^5$	R_g, nm	$A_2/10^{-4}$ cm³·mol·g⁻²	$[\eta]$, dL g⁻¹	L,[c] nm	L_{R_g},[d] nm	d,[e] nm	d_{R_g},[f] nm	h, nm	$(M_zM_{z+1})^{1/2}M_w^{-1}$	$D^0/10^{-7}$ cm² s⁻¹	k_d,[g] mL g⁻¹
2.09 ± 0.10[a]	32.7 ± 2.0	1.92 ± 0.10	1.48								
2.48 ± 0.12	33.2 ± 2.0	2.49 ± 0.13	1.21	97.4	115.0	3.4 3.4*	2.4 2.2*	0.177	1.18	3.31	15.6
1.85 ± 0.09	27.9 ± 1.6	2.33 ± 0.12	0.83	72.6	96.6	3.2 3.8*	1.8 1.9*	0.199	1.33	3.93	15.3
1.55 ± 0.08	23.2 ± 3.0	3.04 ± 0.21	0.64	61.1	80.4	4.2 3.6*	2.4 2.0*	0.197	1.32	4.45	11.0
1.21 ± 0.06	18.0 ± 2.0	1.96 ± 0.13	0.46	47.5	62.3	2.7 3.7*	1.6 2.2*	0.197	1.31	5.18	6.7
0.96 ± 0.05	13.0 ± 2.0	3.24 ± 0.18	0.25	37.7	45.0	4.5 3.9*	3.1 3.0*	0.179	1.19	5.82	23.6
0.47 ± 0.02	*b*	2.88 ± 0.16	0.16	18.5		4.0				8.03	4.8

[a] PSLG-EX. [b] Polymer too small to reliably measure R_g. [c] $L = M_w(0.15\text{ nm})/M_0$. [d] $L_{R_g} = R_g(12^{1/2})$. [e] Calculated using the value of L. Unstarred values computed from $A_2 = \pi N_A dL^2/(4M^2)$. [f] Calculated using the value of L_{R_g}. Unstarred values computed from $A_2 = \pi N_A dL^2/(4M^2)$. Values bracketed by stars computed from the Kirkwood–Riseman expression, $D_0 = kT \ln (L/d_h)/3\pi\eta_0 L$. [g] $\theta = 45°$ data; using third-order cumulant fits.

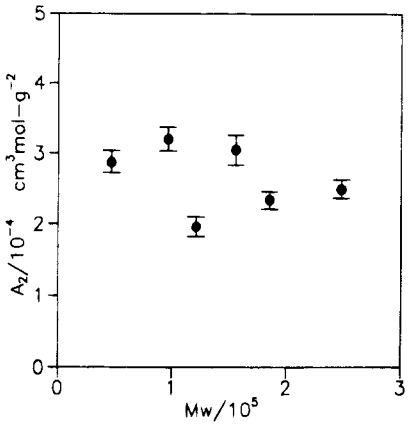

Figure 7. A_2 vs M_w. No systematic dependence of A_2 on M_w is consistent with a rod-like structure in solution.

$$M_0 = (\varrho\pi d_\varrho^{\,2} h N_A)/4 \qquad (2)$$

nm. Agreement between the thermodynamic and density-based diameters depends on the compactness of the side chains; for highly extended, solvent-permeated side chains, one expects $d > d_\varrho$. For PBLG, the two diameters are nearly identical.[61] One might expect a difference for the long PSLG side chains. The large uncertainty surrounding the thermodynamic diameter of the present PSLG samples obscures this difference, but the average value using $L = 0.15M_w/M_0$ significantly exceeds d_ϱ.

Measurements of the PSLG diameter were also made by SYBYL molecular modeling software. Figure 8 shows a PSLG chain of DP = 20 which was energy minimized using the MAXIMIN2 routine with Tripos parameters. The SYBYL model did not take into account solvent interactions, and when the polymer was built, the α-helical conformation was chosen for the model. This means that SYBYL started with the "correct" dimensional values. However, upon minimization SYBYL will "break" or change a conformation if there is strain or unfavorable interactions in the molecule. An estimate of the diameter can be obtained by allowing SYBYL to calculate the distance between opposing terminal CH_3 groups in the side chains. An average of 4.1 ± 0.1 nm was obtained. Measuring the diameter in this manner at the amino terminus of the chain gives 3.4 ± 0.3 nm. SYBYL can also calculate the volume occupied by a compound by calculating the volume that each atom occupies and ignoring "dead space" between the atoms. Using this value of the volume, we can again calculate a solid cylinder diameter of PSLG. PSLG with DP = 20 has a volume of V = 7.467 nm³ according to SYBYL and a length L_s = 3 nm (subscript s stands for SYBYL). The equation for the volume of a cylinder, $V = \pi d_s^2 L_s/4$, yields d_s = 1.8 nm. Since d_s is the diameter of a PSLG rod where all the atoms are "packed" into a cylinder without any empty space, this sets the lower limit for the diameter of PSLG.

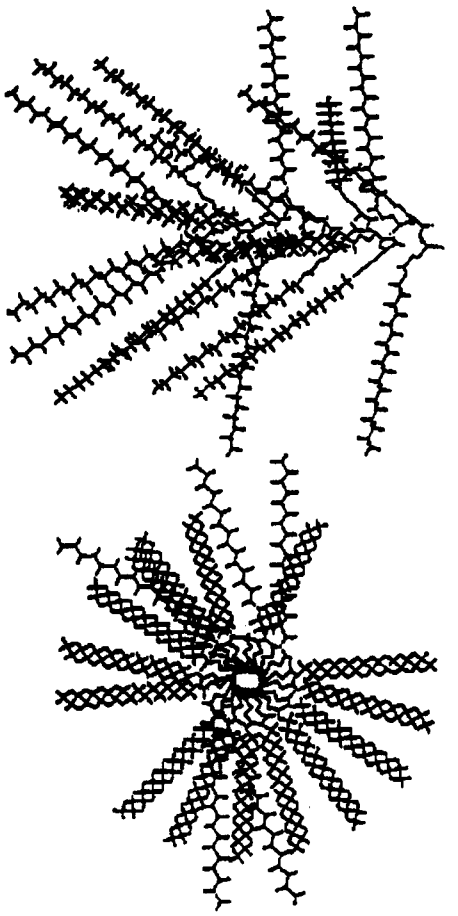

Figure 8. SYBYL molecular model of PSLG (DP = 20). The energy minimization routine used was MAXIMIN2: (upper) side view, amino terminus to the left; (lower) amino terminus end view.

SYBYL also provided a value of h = 0.153 nm for the helical pitch/residue of PSLG. The close agreement with the expected value for an α-helix, 0.15 nm, suggests that

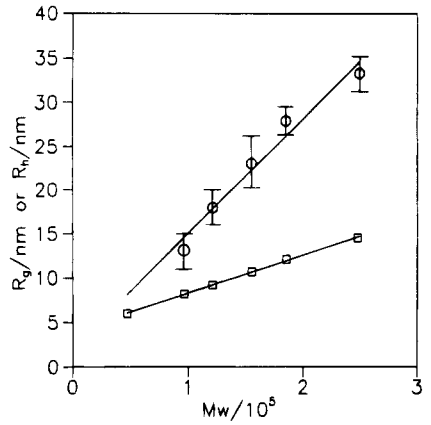

Figure 9. R_g (○) and R_h (□) which increase linearly with M_w. Error bars for R_h are comparable in size to the data points. The linear correlation coefficient is 0.982 for the R_g plot and 0.999 for the R_h plot.

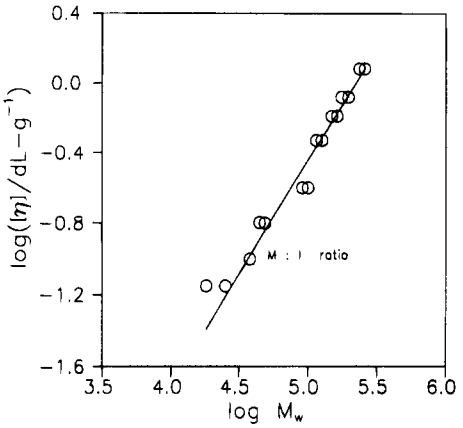

Figure 10. Mark–Houwink relationship for linear PSLG in THF at 30 °C in the range of 20 000–250 000. $[\eta]$ in cm^3/g = $(1.26 \pm 0.3) \times 10^{-5} M^{1.29 \pm 0.09}$.

the stearyl side chains do not perturb the dimensions of the helical backbone. Using experimental R_g values and assuming rod-like behavior of the polymer (i.e., $R_g^2 = L^2/12$), h can be calculated from the relationship $h = R_g(12^{1/2}) \times 382/M_w$. The average value so obtained is $h = 0.19 \pm 0.01$ nm. A plot of R_g vs M_w (Figure 9) will also provide an estimate of h where the slope of the line is $h/M_0(12^{1/2})$. In this way, which sidesteps the problem that a small contribution to R_g is made by the finite rod diameter, a value of $h = 0.175 \pm 0.022$ nm is obtained, in better agreement with the expectation. Other workers[62,63] have evaluated h for PBLG anywhere from 0.085 to 0.22 nm. For the fractionated samples of DeLong and Russo[64] h averaged 0.158 ± 0.003 nm. Molecular weight heterogeneity is mostly to blame for the wide range of reported values and the somewhat high values reported here.

The correlation between molecular weight and intrinsic viscosity, expressed by the Mark–Houwink (M–H) parameters, also indicates an extended shape. The intrinsic viscosity, $[\eta]$, was determined in THF at 30 °C by capillary viscometry and the data used to generate a Huggins plot to obtain $[\eta]$. The Huggins relationships were linear, with both relationships intercepting at nearly the same point on the y-axis. The M–H plot in Figure 10 yields $K = (1.26 \pm 0.3) \times 10^{-5}$ cm^3/g and $a = 1.29 \pm 0.09$ for M_w in the range of 38 000–250 000. The value for a is close to that obtained by a recent reanalysis[65] of Doty's data[61] on PBLG, which yields $a = 1.33 \pm 0.07$. PSLG is probably comparable rigid to

Table 3. GPC Data for Linear PSLG

mol wt[a] light scattering	retention time, min	GPC M_w	GPC M_n	M_w/M_n
248 000	7.70	254 900	90 300	2.82
175 000	7.93	150 600	75 700	1.99
148 000	8.17	156 800	78 900	1.99
126 000	8.40	100 200	64 600	1.55
93 000	8.63	67 200	50 100	1.34
47 000	8.87	51 900	40 900	1.27
38 200[b]	9.33	35 400	31 600	1.12
20 000	10.50	32 500	25 300	1.28

[a] Molecular weights used to calibrate the GPC column. [b] Primary amine initiation. Value calculated from the {M}:{I} ratio.

PBLG. Unfortunately, it is difficult to specify just how rigid that is; the persistence length of PBLG has been measured many times, with values ranging from 70 to over 200 nm.[66–68]

PSLG-EX synthesized by transesterification of commercially available PMLG was also characterized by SLS. The molecular weight supplied by the manufacturer (Sigma) for PMLG was 100 000, giving a calculated R_g (L calculated from M_w and $h = 0.15$ nm) of 27.2 nm and a calculated PSLG molecular weight of about 240 000, assuming complete transesterification. Light scattering results gave $M_w = 209\,500 \pm 4900$ with an R_g of 32.7 ± 0.2 nm and $A_2 = (1.92 \pm 0.103) \times 10^{-4}$ cm^3·mol·g^{-2}. In making these calculations, the dn/dc value for compositionally pure PSLG was used, and copolymer effects[69] were ignored. Results obtained for PSLG-EX were not used in any of the dimension determinations of PSLG. For fundamental work on PSLG, this method of synthesis is not recommended. We have found discrepancies, for example, in the thermal behavior of PSLG-EX compared to PSLG synthesized directly from the monomer.[70] One may also expect, with varying amounts of comonomer present, different degrees of solvent compatibility or side-chain expansion from the backbone.

The major limitation to the above results is the polydispersity of the samples. We estimated the molecular weight distribution of the PSLG samples in two ways, the first being gel permeation chromatography (GPC). Table 3 shows GPC results for the samples in THF using one mixed-bed 10-μm Phenogel column. A single mixed-bed column does not offer optimal separation but does give a quick analysis and permits relative comparisons between samples. The GPC data shown in Table 3 were generated by first making a calibration curve of M_w (from SLS) vs retention time and then analyzing the *same* samples using Nelson Analytical GPC software to give a GPC M_w and apparent polydispersity index M_w/M_n. Under these conditions, all of the polymers had a polydispersity index < 2 except for PSLG-248 000. The narrowest MWD PLSG (apparent $M_w/M_n = 1.12$) was the benzylamine-initiated PSLG with {M}:{I} = 100.

The second way of estimating the molecular weight distribution utilizes the known responses of the various quantities measured by SLS to polydispersity.[69] Many of the dimensional calculations are based on R_g. As mentioned already, light scattering directly measures the z-average of $\langle R_g^2 \rangle$—i.e., $\langle R_g^2 \rangle_z$. The molecular weight corresponding to $(\langle R_g^2 \rangle_z)^{1/2}$ depends upon shape. For rodlike polymers, the geometric mean of M_z and M_{z+1} should be used.[60] For helical rods, $\langle R_g \rangle_z^2 = M_z M_{z+1} h^2/12M_0^2$. It is easily shown that $(M_z M_{z+1})^{1/2}/M_w = 12^{1/2} R_g M_0/hM_w$, where $R_g = (\langle R_g^2 \rangle_z)^{1/2}$. The left-hand side is a polydispersity ratio, albeit an unusual one, that

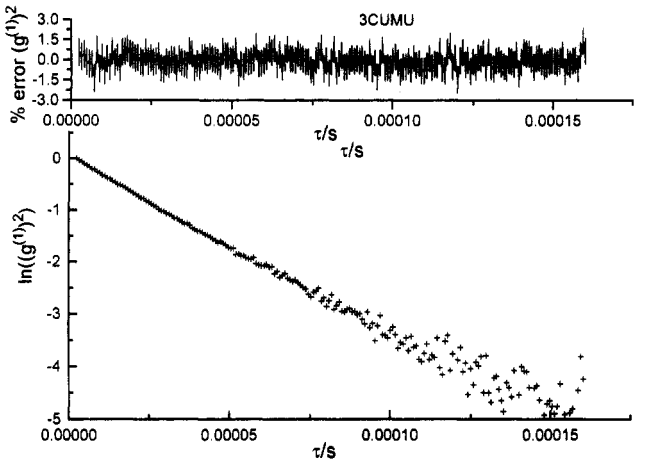

Figure 11. Typical DLS results for a PSLG with $M_w = 96\,000$.

tends toward unity for monodisperse polymers and assumes the value $3^{1/2}$ for a most probable distribution.[64] Using the measured R_g and M_w values and assuming $h = 0.15$ nm, we can compute this polydispersity index for each polymer. Table 2 shows the results; the polymer distributions appear to be sharper than most probable, though hardly sharp in an absolute sense and considerably worse than the PBLG fractions prepared by DeLong and Russo.[64]

Dynamic light scattering (DLS) measurements were performed on the same solutions, in the same cells, prepared for SLS. DLS probes intensity flucuations that arise from thermally stimulated mutual diffusion. The quantity of interest is the electric field autocorrelation function, which under the conditions encountered in a dilute polymer solution at sufficiently low scattering angle is $g^{(1)}(\tau) = e^{-q^2D\tau}$ where D is the mutual diffusion coefficient and $q = 4\pi n \sin(\theta/2)/\lambda_0$ is the magnitude of the scattering vector (n is the solution refractive index, θ is the scattering angle, and λ_0 is the wavelength *in vacuo*). In practice, D was obtained from the slope of a plot of Γ vs q^2 and from the y-intercept of a plot of D_m vs c as shown in Figure 12.

Figure 11 shows a DLS correlation function for PSLG ($M = 96\,000$). The smooth curvature in this semilogarithmic representation of the correlation function suggests a unimodal distribution of moderate width. However, DLS is not very sensitive to low-mass polymers in the presence of larger polymers, which is the expected situation for NCA polymerization according to literature[71] and GPC results; see Figure 3. In the standard cumulants analysis,[31] one fits the semilog representation of Figure 11 to a polynomial curve to obtain the z-average diffusion coefficient. The present results are based on a cubic fit (3CUMU fit). The ratio of the quadratic term, μ_2, to the square of the linear term, Γ, has been used to approximate the molecular weight distribution for rods. Specifically, it has been suggested[72] that $M_w/M_n = 1 + \mu_2/\Gamma^2$. Typical values of M_w/M_n so obtained were 1.2–1.4.

Dynamic light scattering measures the mutual diffusion coefficient, which is essentially the ratio of thermodynamic driving force to hydrodynamic friction resistance.[73] The positive slopes in Figure 12 imply that thermodynamic (excluded volume) interactions, which hasten mutual diffusion as polymer concentration increases, are sufficiently strong to overwhelm the rising mutual friction term. This behavior is common for polymers in good solvents. In studies of PBLG in a good solvent, the initial concentration dependence of D from

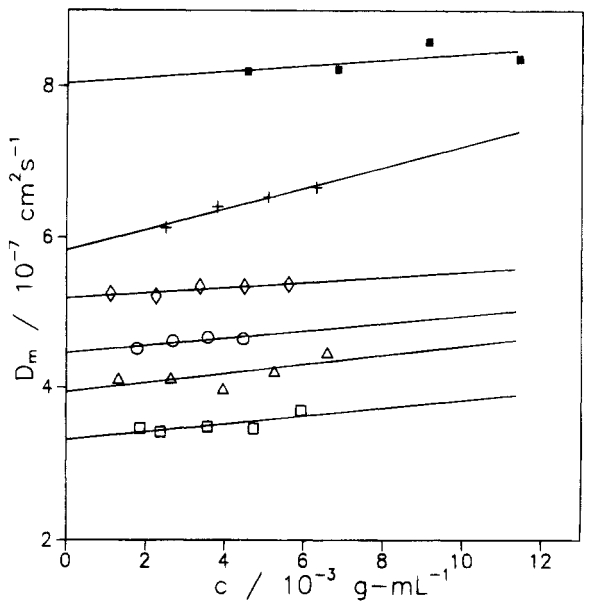

Figure 12. Concentration dependence of diffusion. The slope provides k_d, and the intercept, D^0. The scattering angle was 45°. M = 48 000 (■), 96 000 (+), 121 000 (◇), 155 000 (○), 185 000 (△), and 248 000 (□).

DLS studies was level or, perhaps, even slightly decreasing.[74,75] This was followed by an increase at higher concentrations. At some molecular weights, the initial level/decreasing effect was subtle.[64] Such details are beyond the scope of the present discussion, but close inspection of Figure 12 does show some evidence for level/decreasing initial behavior for the highest two molecular weights which are most expected to exhibit entanglement phenomena. Even for these samples, we do not commit a serious error by writing $D_z = D_{0,z}(1 + k_dc)$, where $D_{0,z}$ is the z-average diffusion coefficient in the limit of zero concentration and k_d is the mutual diffusion viral coefficient. Table 2 contains the values of D_0 and k_d. For these polydisperse samples, the diffusion coefficient scales with molecular weight as $D_{0,z} \sim M_w^{-0.63\pm0.02}$ where we have used only the four points at highest molecular weight (121 000 ≤ M ≤ 248 000). The like result for fractionated PBLG[64] is $D_0 = [(2.75 \pm 1.7) \times 10^{-3}]M^{-(0.78\pm0.05)}$ cm^2 s^{-1}. If ν is the exponent describing the size–mass relationship (e.g., $R_g \sim M^\nu$), then, in a very simple-minded approach, we expect $D_0 \sim M^{-\nu}$ and $[\eta] \sim R_g^3/M \sim M^{3\nu-1}$. The PBLG results are entirely consistent, since $D_0 \sim M^{-0.78}$ and $[\eta] \sim M^{1.33}$, as already noted. The PSLG results do not satisfy these simple scaling relationships, probably because the materials are not sufficiently monodisperse. D_0 is related to the hydrodynamic radius, R_h, by the Stokes–Einstein expression: $D_0 = kT/6\pi\eta_0R_h$ where k is Boltzmann's constant, T is the absolute temperature, and η_0 is the solvent viscosity. Hydrodynamic radii are plotted in Figure 9 alongside the R_g values from SLS. The linear increase with M suggests a stiff polymer, despite the low power law exponents just discussed. Finally, the hydrodynamic diameter, d_h, can be obtained from the Kirkwood–Riseman[76] expression for the diffusion of rods: $D_0 = kT\ln(L/d_h)/3\pi\eta_0L$. In Table 2, these values from DLS are starred and located underneath the values from the virial expansion analysis of SLS data. The average hydrodynamic diameter is 3.7 ± 0.2 nm is L is computed from M_w but only 2.3 ± 0.4 if L is computed from R_g. These numbers are similar to those from the viral coefficient analysis above. More sophis-

ticated treatments by Broersma and others[77] are unwarranted because of the sample polydispersity.

Conclusions

Synthesis of SLGAA from L-glutamic acid and stearyl alcohol was accomplished in reasonable yield by the method of Wasserman.[29] The SLGNCA monomer was readily formed in high yield through the application of triphosgene[12] as a substitute for phosgene gas. High molecular weight PSLG was attainable by the use of low {M}:{I} ratios of sodium methoxide in methanol to a 5−10% solution of SLGNCA in DCM, allowing several days of aging to pass prior to concentration and precipitation of the polymer. A narrower MWD but lower molecular weight PSLG was obtained using primary amine initiation. ^{1}H NMR results revealed a helix−coil transition at about 6% (v/v) TFA. From NMR, SLS, viscosity, and DLS experiments, the approximate dimensions and behavior of PSLG in solution were observed. Preliminary dimensional relationships, such as L and R_g vs M_w, indicate a stiff polymer, as does the Mark−Houwink a value of 1.29. Needed refinements to the structural analysis await more monodisperse samples.

Acknowledgment. Dr. Mazidah Mustafa and Dr. Shoulan Yang provided d*n*/dc measurements. Dr. Mustafa and Dr. Soo Lee also provided help on the measurements of the Zimm plots. This work was supported by NSF Award DMR-8914604 and by Research Corp.

References and Notes

(1) Aharoni, S. M. *Macromolecules* **1979**, *12* (1), 94.
(2) Aharoni, S. M. *Polymer* **1980**, *21*, 1413.
(3) Aharoni, S. M.; Walsh, E. K. *J. Polym. Sci.* **1979**, *17* (5), 321.
(4) Aharoni, S. M. *Polym. Prepr. (Am. Chem. Soc., Div. Polym. Chem.)* **1980**, *21* (1), 209.
(5) Aharoni, S. M. *Polym. Prepr. (Am. Chem. Soc., Div. Polym. Chem.)* **1980**, *21* (1), 211.
(6) Aharoni, S. M. *Macromolecules* **1979**, *12* (3), 537.
(7) Aharoni, S. M. *Macromolecules* **1981**, *14* (1), 222.
(8) Aharoni, S. M.; Walsh, E. K. *Macromolecules* **1979**, *12* (2), 271.
(9) Aharoni, S. M. *Polymer* **1980**, *21*, 21.
(10) Wolfe, J. F.; Loo, B. H.; Arnold, F. E. *Macromolecules* **1981**, *14* (4), 915.
(11) Leuchs, H. *Ber. Dtsch. Chem. Ges.* **1906**, *39*, 857.
(12) Daly, W. H.; Poché, D. *Tetrahedron Lett.* **1988**, *29* (46), 5859.
(13) Leuchs, H.; Manasse, W. *Ber. Dtsch. Chem. Ges.* **1907**, *40*, 3235.
(14) Ben-Ishai, D.; Katchalski, E. *J. Am. Chem. Soc.* **1952**, *74*, 3688.
(15) Curtius, T.; Sieber, W. *Ber.* **1921**, *54*, 1430.
(16) Levy, A. L. *Nature* **1950**, *165*, 152.
(17) Fuchs, F. *Ber. Dtsch. Chem. Ges.* **1922**, *55*, 2943.
(18) (a) Farthing, A. C. *J. Chem. Soc., Part 4*, **1950**, 3213. (b) Coleman, D. *J. Chem. Soc., Part 3*, **1951**, 2294,
(19) Fuller, W. D.; Velander, M. S.; Goodman, M. *Biopolymers* **1976**, *15*, 1869.
(20) Imanishi, Y. *Pure Appl. Chem.* **1981**, *53*, 715.
(21) Sekiguchi, H. *Pure Appl. Chem.* **1981**, *53*, 1689.
(22) Goodman, M.; Peggion, E. *Pure Appl. Chem.* **1981**, *53*, 699.
(23) Watanabe, J.; Fukuda, K.; Gehani, R.; Uematsu, I. *Macromolecules* **1984**, *17*, 1004.
(24) Watanabe, J.; Goto, M.; Nagase, T. *Macromolecules* **1987**, *20* (2), 298.
(25) Watanabe, J.; Ono, E.; Uematsu, I.; Abe, A. *Macromolecules* **1985**, *18* (11), 2141.
(26) Watanabe, J.; Nagase, T. *Polym. J.* **1987**, *10* (6), 781.
(27) Jamil, T.; Russo, P. S.; Negulescu, I.; Daly, W. H.; Schaefer, D. W.; Beaucage, G. *Macromolecules* **1994**, *27* (1), 171.
(28) Eckert, H.; Forster, B. *Angew. Chem., Int. Ed. Engl.* **1987**, *26*, 894.
(29) Wasserman, D.; Garber, J. D.; Meigs, F. M. U.S. Patent 3 285 953, 1966.
(30) DeLong, L. M. Ph.D. Dissertation, Louisiana State University, Baton Rouge, LA, 1990.
(31) Koppel, D. E. *J. Chem. Phys.* **1972**, *57*, 4814.
(32) Weidenheimer, J. F.; Ritter, L.; Richter, F. J. U.S. Patent 2 783 245, 1957.
(33) Sheehan, J. C.; Bolhofer, W. A. *J. Am. Chem. Soc.* **1950**, *72*, 2470.
(34) Dhar, M. M.; Agarwal, K. L. *Steroids* **1964**, *3*, 139.
(35) Block, H. *Poly(γ-benzyl-L-glutamate) and other Glutamic Acid Containing Polymers*; Gordon and Breach: New York, 1983; p 29.
(36) Ledger, R.; Stewart, F. H. C. *Aust. J. Chem.* **1985**, *18*, 1477.
(37) Councler, C. *Ber. Dtsch. Chem. Ges.* **1880**, *13*, 1698.
(38) Idelson, M.; Blout, E. R. *J. Am. Chem. Soc.* **1958**, *80*, 2387.
(39) Shalitin, Y. In *Ring Opening Polymerization*; Frisch, K. C., Ed.; Marcel Dekker: New York, 1969; p 421.
(40) Weingarten, H. *J. Am. Chem. Soc.* **1958**, *80*, 352.
(41) Shalitin, Y.; Katchalski, E. *J. Am. Chem. Soc.* **1960**, *82*, 1630.
(42) Kumar, A. *Indian J. Chem., Sect. B* **1987**, *26B* (7), 634.
(43) Ballard, G. D. H.; Bansford, C. H. *Proc. R. Soc. London* **1954**, *223A*, 495.
(44) Nylund, R. E.; Miller, W. G. *Biopolymers* **1964**, *2*, 131.
(45) Cosani, A.; Peggion, E.; Scoffone, E.; Verdini, A. S. *Makromol. Chem.* **1966**, *97*, 113.
(46) Idelson, M.; Blout, E. R. *J. Am. Chem. Soc.* **1957**, *79*, 3948.
(47) Kricheldorf, H. R. *Makromol. Chem.* **1977**, *178*, 1959.
(48) Goodman, M.; Hutchinson, J. *J. Am. Chem. Soc.* **1966**, *88*, 3627.
(49) Bamford, C. H.; Block, H. In *Polyamino Acids, Polypeptides, and Proteins*; Stahmann, M. A., Ed.; University of Wisconsin Press: Madison, WI, 1963; p 65.
(50) Szwarc, M. *Adv. Polym. Sci.* **1965**, *4*, 1.
(51) Goodman, M.; Arnon, U. *J. Am. Chem. Soc.* **1964**, *86*, 3384.
(52) Peggion, E.; Scoffone, E.; Consani, A.; Portolan, A. *Biopolymers* **1966**, *4*, 695.
(53) Poché, D. S. Ph.D. Thesis, Louisiana State University, Baton Rouge, LA, 1990.
(54) Sakamoto, K.; Akito, O. *Mol. Cryst. Liq. Cryst.* **1987**, *153*, 385.
(55) Miyazawa, T.; Blout, E. R. *J. Am. Chem. Soc.* **1961**, *83*, 712.
(56) Bradbury, E. M.; Crane-Robinson, C.; Goldman, H.; Rattle, H. W. E. *Nature* **1968**, *217*, 812.
(57) Bradbury, E. M.; Cary, P.; Crane-Robinson, C.; Daolillo, T.; Tancredi, T.; Temussi, P. A. *J. Am. Chem. Soc.* **1971**, *93*, 5916.
(58) Smith, J. C.; Woody, R. W. *Biopolymers* **1973**, *12*, 2657.
(59) (a) Zimm, B. H. *J. Chem. Phys.* **1946**, *14*, 164. (b) Schulz, G. V. *Naturforsch.* **1947**, *2A*, 348. (c) Onsager, L. *Ann. N.Y. Acad. Sci.* **1949**, *51*, 627.
(60) Kratochvil, P. In *Light Scattering from Polymer Solutions*; Huglin, M. B., Ed.; Academic Press: New York, 1972.
(61) Doty, P.; Bradbury, J. M.; Holtzer, A. M. *J. Am. Chem. Soc.* **1956**, *78*, 947.
(62) Spach, G.; Freund, L.; Daune, M.; Benoit, H. *J. Mol. Biol.* **1963**, *7*, 468.
(63) Jennings, B. R.; Jerrard, H. G. *J. Phys. Chem.* **1965**, *69*, 2817.
(64) DeLong, L. M.; Russo, P. S. *Macromolecules* **1991**, *24* (23), 6139.
(65) Bu, Z. Ph.D. Dissertation, Louisiana State University, Baton Rouge, LA, 1994.
(66) Yamakawa, H. Stiff-Chain Macromolecules. *Annu. Rev. Phys. Chem.* **1984**, *35*, 23.
(67) Aharoni, S. M. *Macromolecules* **1983**, *16* (11), 1722.
(68) Schmidt, M. *Macromolecules* **1984**, *17* (4), 553.
(69) Kratochvil, P. In *Light Scattering from Polymer Solutions*; Huglin, M. B.; Ed.; Academic Press: New York, 1972; Chapter 7.
(70) Daly, W. H.; Negulescu, I.; Russo, P. S.; Poché, D. S. In *Macromolecular Assemblies in Polymer Systems*; Stroeve, P., Balazs, A., Eds.; ACS Symposium Series 493; American Chemical Society: Washington, DC, 1992; Chapter 23.
(71) Lundberg, R. D.; Doty, P. *J. Am. Chem. Soc.* **1957**, *79*, 3961.
(72) Kubota, K.; Chu, B. *Biopolymers* **1983**, *22*, 1461.
(73) Yamakawa, H. *Modern Theory of Polymer Solutions*; Harper and Row: New York, 1971.
(74) Tracy, M.; Pecora, R. *Macromolecules* **1992**, *25* (1), 337.
(75) Jamil, T.; Russo, P. S. *J. Chem. Phys.* **1992**, *97* (4), 2777−2782.
(76) Riseman, J.; Kirkwood, J. G. *J. Chem. Phys.* **1950**, *18*, 512.
(77) For a review, see: Russo, P. S. In *Dynamic Light Scattering, the Method and Some Applications*; Brown, W., Ed.; Oxford: New York, 1993; p 512.

MA946365J